Enhancing shear thickening

Yasaman Madraki, Sarah Hormozi, Guillaume Ovarlez, Elisabeth Guazzelli, Olivier Pouliquen

Enhancing Shear Thickening

Fatemeh (Yasaman) Madraki[1], Sarah Hormozi[1],
Guillaume Ovarlez[2], Élisabeth Guazzelli[3], Olivier Pouliquen[3]
[1]*Department of Mechanical Engineering,*
Ohio University, Athens, Ohio 45701-2979, USA
[2]*University of Bordeaux, CNRS, Solvay,*
LOF, UMR 5258, 33608 Pessac, France
[3]*Aix-Marseille Univ, CNRS, IUSTI, Marseille, France*

(Dated: February 9, 2017)

Abstract

A cornstarch suspension is the quintessential particulate system that exhibits shear thickening. By adding large non-Brownian spheres to a cornstarch suspension, we show that shear thickening can be significantly enhanced. More precisely, the shear thickening transition is found to be increasingly shifted to lower critical shear rates. This influence of the large particles on the discontinuous shear thickening transition is shown to be more dramatic than that on the viscosity or the yield stress of the suspension.

PACS numbers: 47.57.Gc,83.80.Hj

I. INTRODUCTION

A shear thickening fluid is one in which the viscosity increases with the rate of shear [see e.g. 1–3]. A classical example is a suspension of cornstarch in water which is often used in demonstrations to exhibit the counterintuitive behavior of shear thickening materials. It indeed behaves as a normal liquid if stirred slowly whereas it acts as a solid when agitated or struck forcefully. A person may even walk on a large pool of cornstarch without sinking provided the walking steps are quick and strong enough to cause the shear thickening phenomenon. Cornstarch suspensions exhibit both continuous (CST) and discontinuous shear thickening (DST). At low cornstarch concentration ϕ_{cs}, rheological measurements show a smooth and continuous increase in viscosity with increasing shear rate. As ϕ_{cs} becomes larger, the increase becomes steeper and eventually leads, at a critical shear rate $\dot{\gamma}_c^0$, to an order-of-magnitude discontinuous jump in viscosity or even directly to jamming. DST is observed in the dense suspension regime for $\phi_{cs} \gtrsim 0.36$.

Despite a sustained research attention since the mid-twentieth century, the origin of shear thickening is still not deciphered and remains a matter of active debate [see e.g. 4–8]. A new promising idea points to a transition from a frictionless to a frictional state of the suspension [9–12]. In this scenario, the shear thickening behavior stems from the existence of short-distance repulsive forces between particles. At low shear rate, the repulsion prevents frictional contacts between particles and the suspension behaves as a suspension of frictionless particles. When the shear rate is increased, the stresses on the particles increases and may overcome the repulsive forces. The friction is mobilized at contact and a transition to a frictional rheology then takes place. Within this picture, the discontinuous shear thickening transition occurs when the shear stress imposed to the suspension reaches a critical stress which depends upon the repulsive forces and the particle size. This new theory of friction-induced shear thickening is supported by recent experimental measurements [13–15] which validate model and simulations. Even with these new advances in the understanding of shear thickening, there is still a compelling need to control more precisely the DST transition as this is an important challenge for industries that handle such fluids that can become solid-like, in particular in applications with dampening and shock-absorption such as found in armor composite material [16] and for curved-surface shear-thickening polishing [17]. This paper presents a novel method to enhance shear thickening by adding large non-Brownian spheres to the cornstarch suspension.

More generally, adding particles to a fluid has been shown to enhance its shear viscosity. This

is known for a Newtonian fluid since the seminal work of Einstein demonstrating that the viscosity of the mixture is increased above that of the suspending fluid [18] and this gradually more with increasing particle concentration [19]. As the jamming transition is approached, steric hindrance becomes dominant. Particle fluctuating motions then become more intense and collective, leading to a divergence of the viscosity [20, 21]. The enhancement effect is also observed when adding non-Brownian particles to a non-Newtonian matrix. In the case of a viscoplastic fluid, adding spherical particles induces an increasingly enhancement of the viscosity (or more precisely the consistency) and the yield stress [22–24]. The intensification of these rheological quantities has been also seen for concentrated colloidal dispersions exhibiting a weak shear-thinning followed by continuous shear thickening [25], as well as for shear-thinning polymer solutions and shear-thickening cornstarch suspension (but only investigated in the regime of CST) [26]. Theoretically, the rheological enhancement caused by adding large particles can be addressed by homogenization approaches [see e.g. 22]. The addition of large particles to a fluid increases locally the shear rates in the fluid, an effect sometimes refers to as a lever effect and described by introducing a lever function relating the magnitude of the local shear rate to the macroscopic shear rate imposed to the whole suspension mixture. The objective of the present work is to study how adding large spherical particles to a dense cornstarch suspension leads to a progressive shift of the DST transition to lower critical shear rates and to investigate how this effect is related to the rheological enhancement also observed.

II. MATERIALS AND METHODS

A. Particles and fluid

The cornstarch (73% Amylopectin and 27% Amylose from Sigma Aldrich, USA) used in the experiments consisted of irregularly-shaped particles ranging from $5-20\ \mu m$ with an average diameter $d_{cs} \approx 13\ \mu m$ and a density 1.68 g·cm^{-3}, see figure 1(b). The suspending fluid, a 54 wt% solution of cesium chloride (Cabot high purity grade from Sigma Aldrich, USA) in distilled water, was chosen to match the density of these particles. The cornstarch suspensions were prepared by carefully mixing the cornstarch particles with the suspending fluid at different volume fractions ϕ_{cs} ranging from 0.10 to 0.44. Large non-Brownian particles with volume fraction ϕ_p ranging from 0.05 to 0.35 were then added to this cornstarch suspension. We used $\phi_{cs} = V_{cs}/V_t(1-\phi_p)$ and

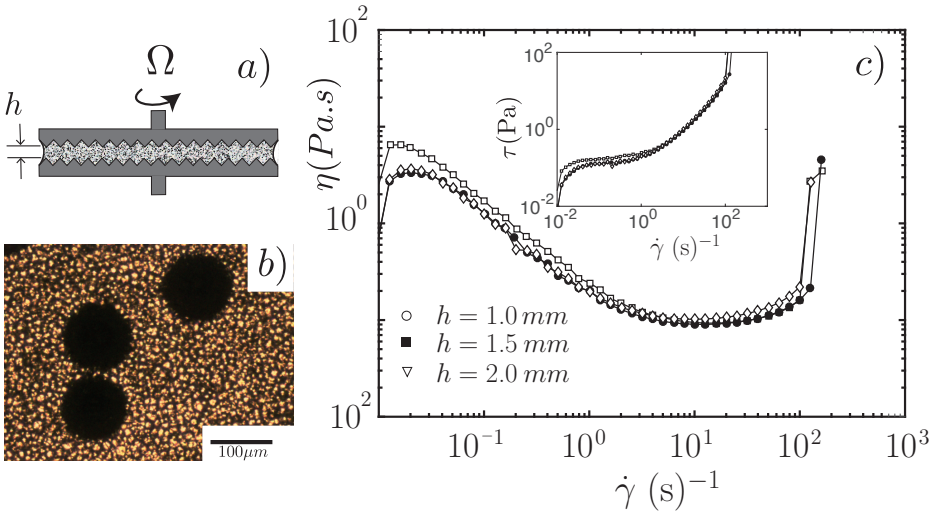

FIG. 1: (a) Sketch of the plate-plate rheometer exhibiting the manufactured grooves. (b) Micrograph of PMMA and cornstarch particles. (c) Viscosity η (Pa $\cdot$ s) versus shear rate $\dot{\gamma}$ (s^{-1}) for different gap sizes h with a cornstarch suspension at $\phi_{cs} = 0.40$. The inset shows the corresponding shear stress τ (Pa) versus shear rate $\dot{\gamma}$ (s^{-1}) for the same gap sizes.

$\phi_p = V_p/V_t$ with V_{cs}, V_p and V_t the volumes of cornstarch, of large particles, and of the whole suspension, respectively. These definitions for the concentrations differed from those usually adopted for bidisperse suspensions. The large particles were Polymethyl methacrylate (PMMA) spheres (Cospheric, USA) of diameter $d_s \approx 106 - 125$ μm, see figure 1(b). These PMMA particles were silver coated to ensure a density of 1.34 g·cm^{-3} which was closest as possible to that of the cornstarch suspension in order to avoid significant sedimentation effect. These large particles were insensitive to Brownian motion and colloidal interactions. Additional experiments were performed using large particles of different sizes (of diameters ranging from $d_p \approx 45 - 355$ μm) but for non-coated PMMA particles (density 1.20 g·cm^{-3}).

B. Rheological methods

The rheological measurements were conducted with a DHR-3 rotational rheometer (TA Instruments) using a 40 mm (diameter) serrated parallel plate geometry with 90 degree V-shaped grooves of height 0.5 mm and width 1 mm. This geometry eliminated wall slip effect, see figure 1(a). In a typical experiment, the desired amount of material was sandwiched between the two crosshatched plates and the rheological device delivered the torque C and the rotation rate Ω yielding to the

determination of the maximum shear stress $\tau = 2C/\pi R^3$ and the maximum shear rate $\dot{\gamma} = \Omega R/h$, and consequently to the effective viscosity $\eta = \tau/\dot{\gamma}$.

Before the experiments were carried out, different tests were performed. A first important test was to check that the rheological measurements were independent of the size of the gap between the plates. This gap dependency was found to be very sensitive to the roughness of the plates as well as to whether the surplus of material around the plates was removed or not. We found that using crosshatched plates and trimming carefully the surplus of material around the plates produced gap-independent measurements in agreement with the experiments of [5], as exhibited in figure 1(c) for a cornstarch suspension at $\phi_{cs} = 0.40$ (see the next paragraph for the description of the rheological curve). A gap size of $h = 1.5$ mm was then chosen for most of the experiments. The second test concerned the reproducibility of the rheological properties of the suspensions. We obtained identical rheological measurements within an accuracy of 15% using different batches of suspensions prepared in the same way or the same batch for different tests but the same day. Last, we checked the time dependency of the experiments by varying the time of the shear rate ramp. No significant differences were observed for a total time of the experiments ranging between 60 and 360 s. This test was also performed when large particles were added to the cornstarch suspensions. A total time of 180 s was chosen for all the experiments for which the influence of sedimentation was found to be inconsequential.

III. EXPERIMENTAL RESULTS

A. Rheological observations

The rheological results for pure cornstarch suspensions are presented in figure 1(c) for $\phi_{cs} = 0.40$ and in figure 2(a) and 2(b) for $0.33 \lesssim \phi_{cs} \lesssim 0.44$. At low $\dot{\gamma}$, the rheology presents a plateau in shear stress, which can be interpreted as a yield stress, τ_y, as evidenced in the inset of figure 1(c). In terms of viscosity, the response is shear thinning as the viscosity η is seen to decrease with increasing $\dot{\gamma}$ until it reaches a minimum plateau η_p, see figure 2(a). For larger $\dot{\gamma}$, continuous (CST) and discontinuous shear thickening (DST) are observed depending upon the cornstarch volume fraction ϕ_{cs}. For $\phi_{cs} \lesssim 0.36$, η smoothly increases with $\dot{\gamma}$ after the minimum Newtonian plateau, whereas for larger ϕ_{cs} a discontinuous jump in η is observed at a critical shear rate $\dot{\gamma}_c^0$. As ϕ_{cs} is increased, the critical shear rate $\dot{\gamma}_c^0$ which characterizes the onset of DST for pure cornstarch

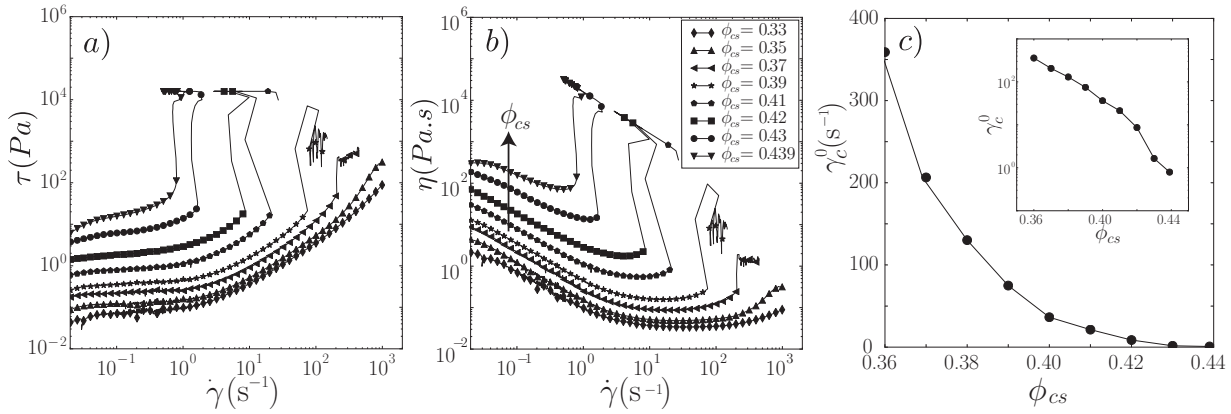

FIG. 2: (a) Shear stress τ (Pa) and (b) viscosity η (Pa $\cdot$ s) versus shear rate $\dot{\gamma}$ (s^{-1}) for pure cornstarch suspensions at different ϕ_{cs}. (c) DST critical shear rate $\dot{\gamma}_c^0$ (s^{-1}) versus ϕ_{cs}. The inset shows the same plot in semi-log scale.

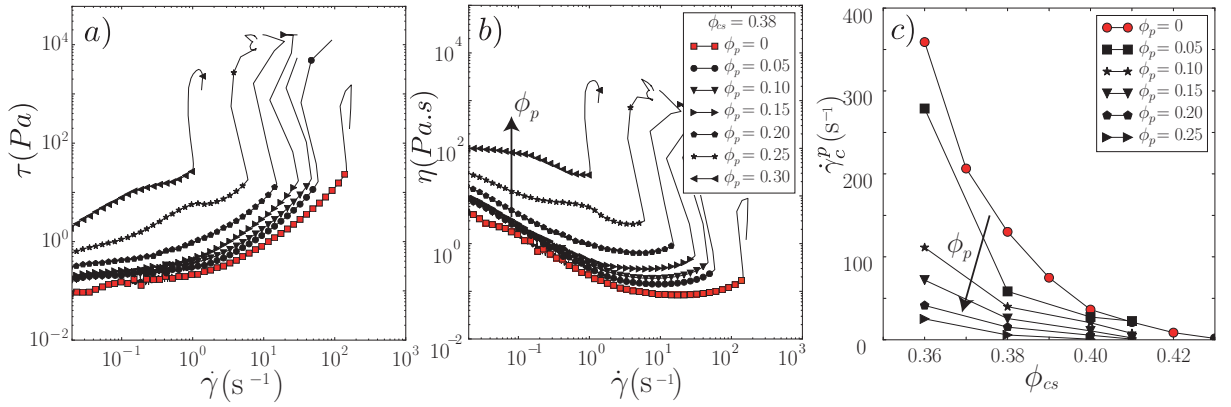

FIG. 3: (a) Shear stress τ (Pa) and (b) viscosity η (Pa $\cdot$ s) for a mixture of silver-coated PMMA spheres and a cornstarch suspension at $\phi_{cs} = 0.38$ for different particle volume fraction ϕ_p. (c) DST critical shear rate $\dot{\gamma}_c^p$ (s^{-1}) versus ϕ_{cs} at different ϕ_p. The red symbols correspond to the data for pure cornstarch suspensions ($\phi_p = 0$).

suspensions is shown to decrease, see figure 2(c), and the minimum Newtonian viscosity η_p is seen to increase, see figure 2(b). Note that the data obtained after the occurrence of DST are not reliable since fracturing and ejection of the material is observed at the edge of the plate-plate device.

Adding large particles to a cornstarch suspension (at constant ϕ_{cs}) has dramatic effects on the rheological behavior and in particular on the DST transition as shown in figures 3(a) and 3(b) for $\phi_{cs} = 0.38$. While the critical shear stress seems to be only slightly affected by this addition

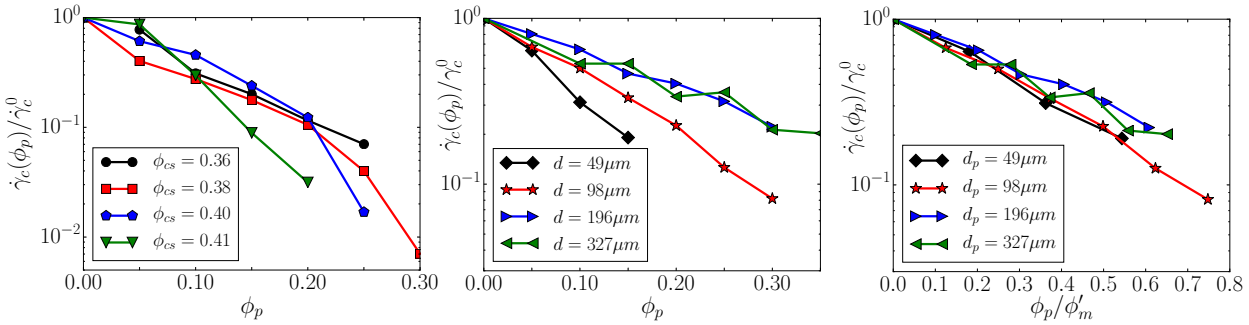

FIG. 4: (a) Critical shear rate $\dot{\gamma}_c^p$ normalized by the critical shear rate for pure cornstarch $\dot{\gamma}_p^0$ as a function of the large particle concentration ϕ_p for different cornstarch concentration ϕ_{cs}. (b) Normalized critical shear rate as a function of ϕ_p for different diameter d_p of large particles for $\phi_{cs} = 0.4$. (c) Same data as (b) but plotted by rescaling ϕ_p using ϕ_m'.

of large particles, see figure 3(a), the effective viscosity of the mixture η is overall increased, see figure 3(b), as seen previously [25, 26]. More strikingly, the DST transition is moved to lower shear rate with increasing particle volume fraction ϕ_p, see figure 3(b). This behavior is systematically observed in the range $0.36 \lesssim \phi_{cs} \lesssim 0.41$. The critical shear rates $\dot{\gamma}_c^p$ which characterize the onset of DST for the mixture of large particles and cornstarch suspensions at different ϕ_p are plotted versus ϕ_{cs} in figure 3(c). This graph clearly evidences the shift of the DST transition to lower shear rate with increasing ϕ_p with an upper bound curve given by that for the pure cornstarch suspension ($\phi_p = 0$ in red) taken from figure 2(c), i.e. the curve $\dot{\gamma}_c^0(\phi_{cs})$.

In the following, we first provide a systematic investigation of the shift in critical shear rate and then discuss the effect of adding particles on the critical shear stress.

B. The shift in the critical shear rate

We examine first the critical shear rates $\dot{\gamma}_c^p$ for the mixture of silver-coated PMMA spheres (of diameter $d_s \approx 106 - 125$ μm) and a cornstarch suspension at different ϕ_{cs} and ϕ_p. Normalizing the critical shear rate $\dot{\gamma}_c^p$ for the mixture of large particles and cornstarch suspensions by the critical shear $\dot{\gamma}_c^0$ for the pure cornstarch suspension leads to a good collapse of the data onto a single master curve as evidenced in figure 4(a) where $\dot{\gamma}_c^p/\dot{\gamma}_p^0$ is plotted against ϕ_p. The dynamics of the dense suspension mixture thus mainly depends on the large particle volume fraction ϕ_p. To complete this rheological analysis and study the role of the aspect ratio between the large spheres and the cornstarch particles, experiments were also performed using large particles of different sizes.

It was however not possible to obtain coated PMMA particles of different sizes. Therefore, we used non-coated PMMA particles (of diameters ranging from ≈ 49 to 327 μm) with the drawback of having a larger mismatch in density. In figure 4(b), the critical shear rates $\dot{\gamma}_c^p$ for the mixture normalized by the critical shear $\dot{\gamma}_c^0$ for the pure cornstarch suspension are plotted as a function of the volume fraction for four different sizes, showing a clear influence of the size d_p of the large particles. The shift to lower shear rate when adding particles is more pronounced when the size of the large particles is decreased, i.e. when the ratio of the large particles to the cornstarch particles is diminished. This influence of the particle size ratio may be related to loosening effects in suspensions consisting of polydisperse particles, i.e. the change in maximum packing volume fraction (ϕ_m) of large particles (PMMA or silver-coated PMMA) due to presence of small particles (cornstarch grains)[27]. If we naively consider that two large particles are always separated by a cornstarch grain even in the closest packing, the new maximum packing volume fraction becomes $\phi_m{}' = \phi_m d_p^3/(d_p + d_{cs})^3$. When the data of figure 4(b) are replotted by rescaling the volume fraction ϕ_p using $\phi_m{}'$, the curves obtained for different particle sizes collapse onto a master curve as evidenced in figure 4(c). This collapse seems to substantiate the idea that the dynamics of the dense suspension mixture is mainly controlled by steric constraints.

C. Influence on the critical shear stress

Whereas adding large particles to a cornstarch suspension dramatically shift the critical shear rate to lower values, the effect is of lesser importance on the critical shear stress, as evidenced in figure 3(a). The DST is observed to occur at a critical stress ≈ 20 Pa. This critical value is in agreement with the experiments of [5] for pure cornstarch suspensions similar to those used in the present study. Note that a lower value of ≈ 5 Pa is found by [15] using similar Sigma Aldrich cornstarch but suspended in a (not so closely density matched) fluid obtained by adding glycerol into the water phase. We systematically measured the critical stress at which the DST transition occurs for different cornstarch concentrations ϕ_{cs}, different large particle concentration ϕ_p, and different particle size ratio. The resulting data are recapitulated in figure 5. The critical stress τ_c^p normalized by the critical value for pure cornstarch τ_c^0 is plotted for all data as a function of the rescaled volume fraction $\phi_p/\phi_m{}'$. The experimental data are seen to collapse onto a single curve. The critical stress is approximately constant and equal to the critical stress for pure cornstarch at low volume fractions but begins to increase when $\phi_p/\phi_m{}' \gtrsim 0.5$.

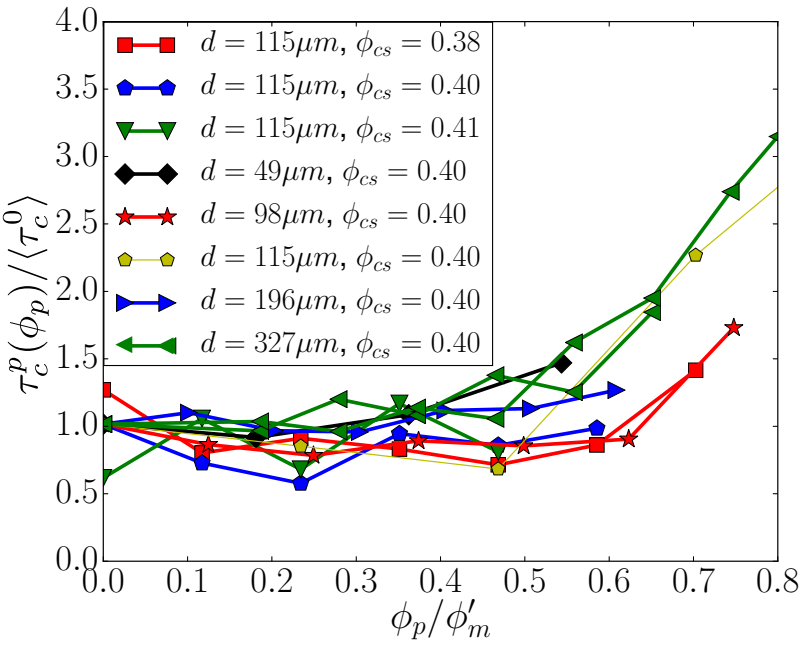

FIG. 5: Critical stress $\tau_c^p(\phi_p)$ at the DST transition normalized by the averaged critical stress for pure cornstarch ($\langle\tau_c^0\rangle = 20.8$ Pa) as a function of the rescaled volume fraction ϕ_p/ϕ'_p for data corresponding to various ϕ_{cs} and d_p.

This observation can be rationalized by the following understanding of the rheology of non colloidal rigid suspensions. At low volume fraction, while it is enhanced by the particles, the bulk stress of a suspension remains purely of hydrodynamic nature and is entirely carried by the suspending-fluid phase. The average stress experienced by the interstitial cornstarch is thus equal to the suspension stress. Assuming that the DST transition occurs at a constant stress in the cornstarch then means that DST occurs at a constant stress for the whole suspension, at least at low particle volume fraction ϕ_p. However, at larger volume fraction, contact can occur between the large particles, and the bulk stress is now carried in part by the large-particle phase and not solely by the suspending-fluid phase. This may explain the increase of the critical stress for DST at larger volume fraction, as in this regime the stress experienced by the cornstarch suspension is now smaller than the total stress applied to the mixture.

The observation of a quasi constant critical shear stress provides a simple interpretation for the lowering of the critical shear rate for the DST transition. Adding large particles enhances the viscosity, implying that the critical shear rate decreases in order to keep the critical stress constant. However, as discussed in the following section, the interpretation of the DST in terms of a constant

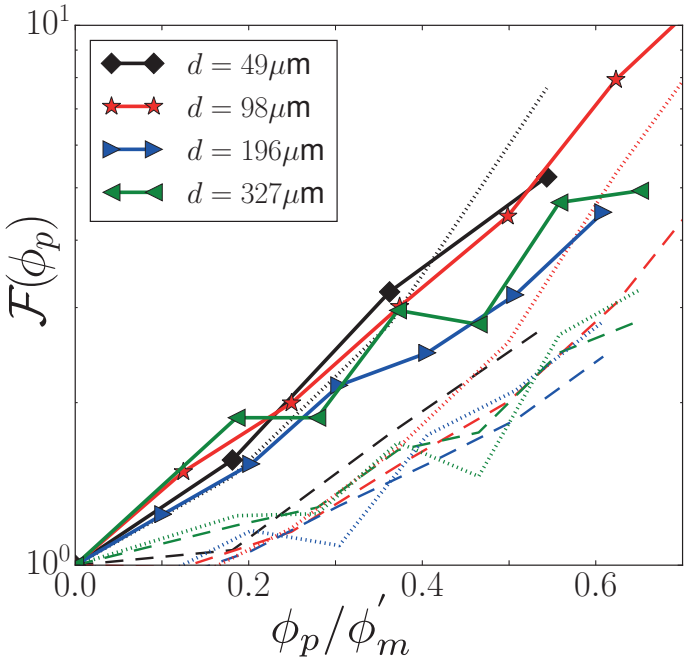

FIG. 6: Estimate of the lever function $\mathscr{F}(\phi_p)$ based on the DST shift $\mathscr{F}^{DST}(\phi_p) = \dot{\gamma}_c^0/\dot{\gamma}_c^p$ (solid lines and symbols), the viscosity shift $\mathscr{F}^{\eta_p}(\phi_p) = \sqrt{\eta_p(\phi_p)/[\eta_p(0)(1-\phi_p)]}$ (dashed lines), and yield stress shift $\mathscr{F}^{\tau_y}(\phi_p) = \tau_y(\phi_p)/\tau_y(0)(1-\phi_p)$ (dotted lines) versus ϕ_p versus ϕ_p/ϕ_m'.

critical shear stress raises several questions when compared with energetic arguments developed in homogenization approaches.

IV. INTERPRETATION IN TERMS OF A LOCAL SHEAR RATE

To analyze and interpret the rheology of suspensions in non-Newtonian fluids, a useful concept is that of local shear rate $\dot{\gamma}_{local}$. The interstitial fluid between the particles experienced a very fluctuating velocity field, and the typical magnitude of the shear rate, called the local shear rate $\dot{\gamma}_{local}$ in the following, is larger than the macroscopic shear rate $\dot{\gamma}$ applied to the suspension because of the indeformability of the large particles. This amplification can be described by introducing a lever function $\mathscr{F}(\phi_p)$ relating the local to the macroscopic shear rate such as $\dot{\gamma}_{local} = \dot{\gamma}\mathscr{F}(\phi_p)$ with the underlying assumption that $\mathscr{F}$ only depends on ϕ_p [20, 22, 23].

The present study of the shift of the critical shear rate at which DST occurs provides a direct estimation of the lever function. The DST should be obtained when $\dot{\gamma}_{local}$ reaches the critical values for pure cornstarch $\dot{\gamma}_c^0$ and therefore when the macroscopic shear rate $\dot{\gamma}$ reaches $\dot{\gamma}_c^0/\mathscr{F}(\phi_p)$.

The lever function estimated from DST is then simply given by the ratio $\mathscr{F}^{DST} = \dot{\gamma}_c^0/\dot{\gamma}_c^p$. These data are plotted in figure 6 as a function of the normalized volume fraction of large particle ϕ_p/ϕ_m' (solid lines and symbols). The good collapse of all data for different large particles and different cornstarch concentrations seems to substantiate the idea that the dynamics of the dense suspension mixture is mainly controlled by steric constraints and thus only depends on the large particle volume fraction ϕ_p.

In addition, the present rheological measurements provide two others ways to estimate the lever function from the shift in rheological properties prior DST, in particular the shift in plateau viscosity $\eta_p(\phi_p)$ and the shift in yield stress $\tau_y(\phi_p)$. The first estimate is derived from an energetic argument stipulating that the dissipation in the suspension is equal to the dissipation in the suspending fluid (which means that contact between the large particles is supposed to be negligible), i.e. $\eta_p(\phi_p)\dot{\gamma}^2 = (1-\phi_p)\eta_p(0)\dot{\gamma}_{local}^2$. This lead to the estimate of the lever function based on the viscosity: $\mathscr{F}^{\eta_p}(\phi_p) = \sqrt{\eta_p(\phi_p)/[\eta_p(0)(1-\phi_p)]}$. The second estimate is obtained again by writing the dissipation at low shear rate when the stress is given by the yield stress: $\tau_y(\phi_p)\dot{\gamma} = (1-\phi_p)\tau_y(0)\dot{\gamma}_{local}$ leading to the lever function based on the yield stress: $\mathscr{F}^{\tau_y}(\phi_p) = \tau_y(\phi_p)/\tau_y(0)(1-\phi_p)$. We have computed these two estimates of the lever function from the rheological curves, $\eta_p(\phi_p)$ being inferred as the minimum plateau viscosity and $\tau_y(\phi_p)$ as the shear stress at $\dot{\gamma} = 0.04\ \mathrm{s}^{-1}$. These two alternative estimates of $\mathscr{F}(\phi_p)$ are also plotted in figure 6 (dashed and dotted lines). They are both in very good agreement and again confirm the sole dependance on the large particle volume fraction ϕ_p.

While these three evaluations of $\mathscr{F}(\phi_p)$ present an increase with increasing large particle volume fraction ϕ_p, they do not match completely. Both estimates of the lever function from viscosity shift (dashed lines) and yield stress shift (dotted lines), $\mathscr{F}^{\eta_p}(\phi_p)$ and $\mathscr{F}^{\tau_y}(\phi_p)$ respectively, are similar whereas the predictions from the DST shift (solid lines and symbols), $\mathscr{F}^{DST}(\phi_p)$, are systematically larger. The influence of the large particles on the DST is clearly more dramatic than that on the viscosity or the yield stress. This discrepancy shows that a simple mean field argument based on a single scalar estimate of the local shear rate is not sufficient to capture the observed rheology and that the DST may be controlled by the extreme values of the local shear rate distribution. It is indeed sufficient to have a percolating jamming network within the interstitial fluid to block macroscopically the mixture.

V. CONCLUSION

In conclusion, we have shown that adding large non-Brownian particles to a cornstarch suspension moves the DST transition to lower critical shear rates providing a method for controlling shear thickening properties by simply varying the concentration of the large particles. The effective plateau viscosity of the mixture prior DST is observed to increase as seen previously [25, 26]. The critical stress for the DST transition is much less affected as it is seen to be approximately constant and equal to that for pure cornstarch in a relative wide range of concentrations of large particles before presenting some increase for larger concentrations.

Interpreting our results in terms of a local shear rate, i.e. stipulating that the presence of large particles enhances the shear rate in the suspending fluid, exhibits a difference between the influence of the large particles on the DST and on the bulk rheology. The local shear rate estimated from the shift in the DST transition is larger than the local shear rate estimated from the shift in viscosity. A simple interpretation in terms of a single estimate of the local shear is thus not appropriate, which may suggest that the DST transition mobilizes the extreme values of the local shear rate distribution while the plateau viscosity (or more generally the bulk rheology prior DST) involves the averaged value. These observations raise questions that require theoretical studies going beyond mean field approaches in order to tackle thoroughly these nonlinear rheological systems.

ACKNOWLEDGMENTS

This work is undertaken under the auspices of the ANR project 'Dense Particulate Systems' (ANR-13-IS09-0005-01), the 'Laboratoire d'Excellence Mécanique et Complexité' (ANR-11-LABX-0092), and the 'Initiative d'Excellence' A*MIDEX (ANR-11-IDEX-0001-02) as well as the NSF Grant No. CBET-1554044-CAREER. We thank Dr. David F. J. Tees (Department of Physics and Astronomy, Ohio University) for his assistance on the suspensions micrography.

---

[1] H. A. Barnes, Shear-Thickening (Dilatancy) in Suspensions of Nonaggregating Solid Particles Dispersed in Newtonian Liquids, J. Rheol. **33**, 329 (1989).

[2] J. Mewis and N. J. Wagner, *Colloidal Suspension Rheology* (Cambridge University Press, 2011).

[3] E. Brown and H. M. Jaeger, Shear thickening in concentrated suspensions: phenomenology, mechanisms and relations to jamming, Rep. Prog. Phys. **77**, 046602 (2014).

[4] R. L. Hoffman, Discontinuous and dilatant viscosity behavior in concentrated suspensions. II. Theory and experimental tests, J. Colloid Interface Sci. **46**, 491 (1974).

[5] A. Fall, N. Huang, F. Bertrand, G. Ovarlez, and D. Bonn, Shear Thickening of Cornstarch Suspensions as a Reentrant Jamming Transition, Phys. Rev. Lett. **100**, 018301 (2008)

[6] N. J. Wagner and J. Brady, Shear thickening in colloidal dispersions, Physics Today, **62**, 27 (2009).

[7] A. Fall, A. Lemaitre, F. Bertrand, D. Bonn, and G. Ovarlez, Shear Thickening and Migration in Granular Suspensions, Phys. Rev. Lett. 105, 268303 (2010).

[8] E. Brown and H. M. Jaeger, The role of dilation and confining stresses in shear thickening of dense suspensions, J. Rheol. **56**, 875 (2012).

[9] N. Fernandez, R. Mani, D. Rinaldi, D. Kadau, M. Mosquet, H. Lombois-Burger, J. Cayer-Barrioz, H. J. Herrmann, N. D. Spencer, and L. Isa, Microscopic Mechanism for Shear Thickening of Non-Brownian Suspensions, Phys. Rev. Lett. **111**, 108301 (2013).

[10] R. Seto, R. Mari, J. F. Morris, and M. M. Denn, Discontinuous Shear Thickening of Frictional Hard-Sphere Suspensions Phys. Rev. Lett. **111**, 218301 (2013).

[11] M. Wyart and M. E. Cates, Discontinuous Shear Thickening without Inertia in Dense Non-Brownian Suspensions, Phys. Rev. Lett. **112**, 098302 (2014).

[12] R. Mari, R. Seto, J. F. Morris, and M. M. Denn, Shear thickening, frictionless and frictional rheologies in non-Brownian suspensions, J. Rheol. 58, 1693 (2014).

[13] Guy, B. M., Hermes, M., and Poon, W. C. K, Towards a Unified Description of the Rheology of Hard-Particle Suspensions. Phys. Rev. Lett. **115**, 088304?5 (2015).

[14] Lin, N. Y. C., Guy, B. M., Hermes, M., Ness, C., Sun, J., Poon, W. C. K., and Cohen, I., Hydrodynamic and Contact Contributions to Continuous Shear Thickening in Colloidal Suspensions. Phys. Rev. Lett., **115**, 228304?5 (2015).

[15] Hermes, M., Guy, B. M., Poon, W. C. K., Poy, G., Cates, M. E., and Wyart, M. Unsteady flow and particle migration in dense, non-Brownian suspensions. Journal of Rheology, **60**, 905?916 (2016).

[16] Y. S. Lee, E. D. Wetzel, and N. J. Wagner, The ballistic impact characteristics of Kevlar woven fabrics impregnated with a colloidal shear thickening fluid, J. Mater. Sci. **38**, 2825 (2003).

[17] M. Li, B. Lyu, J. Yuan, C. Dong, and W. Dai, , Shear-thickening polishing method, Int. J. Mach. Tools Manuf., **94**, 88 (2015).

[18] A. Einstein, Über die von der molekularkinetischen Theorie der WŁrme geforderte Bewegung von in ruhenden Flssigkeiten suspendierten Teilchen, . Annalen der Physik Ann. Phys. (Berlin) **322**, 549 (1905).

[19] J. J. Stickel and R. L. Powell, Fluid mechanics and rheology of dense suspensions, Annu. Rev. Fluid Mech. **37**, 129 (2005)

[20] E. Lerner, G. Düring, and M. Wyart, A unified framework for non-Brownian suspension flows and soft amorphous solids, PNAS **109**, 4798 (2012).

[21] B. Andreotti, J.-L. Barrat, and C. Heussinger, Shear Flow of Non-Brownian Suspensions Close to Jamming, Phys. Rev. Lett. **109**, 105901 (2012).

[22] X. Chateau, G. Ovarlez, and K. L. Trung, Homogenization approach to the behavior of suspensions of noncolloidal particles in yield stress fluids, J. Rheol. **52**, 489 (2008)

[23] S. Dagois-Bohy, S. Hormozi, É. Guazzelli, and O. Pouliquen, Rheology of dense suspensions of non-colloidal spheres in yield-stress fluids, J. Fluid Mech. **776**, R2 (2015).

[24] G. Ovarlez, F. Mahaut, S. Deboeuf, N. Lenoir, S. Hormozi, and X. Chateau, Flows of suspensions of particles in yield stress fluids, J. Rheol. **59**, 1449 (2015);

[25] C. D. Cwalina and N. J. Wagner, Rheology of non-Brownian particles suspended in concentrated colloidal dispersions at low particle Reynolds number, J. Rheol. **60**, 47 (2016).

[26] M. Liard, N. S. Martys, W. L. George, D. Lootens, and P. Hebraud, Scaling laws for the flow of generalized Newtonian suspensions, J. Rheol. **5**, 1993 (2014).

[27] X. Chateau, in *Understanding the rheology of concrete* (Woodhead Publishing Series in Civil and Structural Engineering, 2012).